Chapter 11

Development of Graphical Solution to Determine Optimum Hollowness of Hollow Cylindrical Roller Bearing Using Elastic Finite Element Analysis

P.H. Darji and D.P. Vakharia

Additional information is available at the end of the chapter

http://dx.doi.org/10.5772/46160

1. Introduction

Technological progress creates increasingly arduous conditions for rolling mechanisms. Advances in many fields including gas turbine design, aeronautics, space and atomic power, involve extreme operating speeds, load, temperatures, environments which increases power and load on machinery and demand high strength to weight ratio of the rolling element bearings. Also bearing stiffness is an important parameter in the designing. Bearing design calculations require a good understanding of the Hertzian contact stress due to which high stress concentration is produced which greatly influence the fatigue life and dominate the upper speed limits as in the case of solid rolling elements. Since being originally introduced, cylindrical rolling element bearings have been significantly improved, in terms of their performance and working life. A major objective has been to decrease the Hertz contact stresses at the roller–raceway interfaces, because these are the most heavily stressed areas in a bearing. It has been shown that bearing life is inversely proportional to the stress raised to the ninth power (even higher). Whereas making the rollers hollow which are flexible enough reduces stress concentration and finally increase the fatigue life of bearing.

Investigators have proposed that under large normal loads a hollow element with a sufficiently thin wall thickness will deflect appreciably more than a solid element of the same size. An improvement in load distribution and thus load capacity may be realized, as well as contact stress is also reduced considerably by using a bearing with hollow rollers. Since for hollow roller bearing no method is available for the calculation of hollowness, contact stresses and deformation. The contact stresses in hollow members are often calculated by using the same equations and procedures as for solid specimens. This approach seems to be incorrect.

Initially in the present work author has carried out sufficient literature review (Somasundar & Krishnamurthy, 1984; Harris & Aaronson, 1967; Bamberger, Parker & Dietrich, 1976; Bhateja & Hahn, 1980; Murthy & Rao, 1983; Hong & Jianjun, 1998; Zhao, 1998; Yangang, Raj & Qingyu, 2004; Darji & Vakharia, 2008) and market survey to understand the practical application of hollow cylindrical roller bearing and its advantages in comparison with solid roller bearing. It is concluded that bearing manufacturer are production these type of bearing as per the requirement, but no standard formula or catalogue is available through which user can directly select hollow cylindrical roller bearing. Thus no standard formula (method) is available to find the optimum hollowness for the given loading condition and dimensions of bearing. Hollowness of the roller bearing is mainly dependent of applied load, dimensions of roller and endurance limit of the material used. Calculation of exact contact pressure for the hollow roller requires a finite element approach, and this has not been carried out yet. Present work is aimed to identify optimum hollowness irrespective of the geometry of the bearing and applied load.

To meet the requirement, in the first part of the present work contact analysis has been carried out for contact between roller and flat. Dimensions of the rollers are calculated using equation of equivalent diameter corresponding to the five different cylindrical roller bearing i. e. 2206, 2210, 2215, 2220 and 2224 to get the large data range. Value of applied load is taken from minimum to maximum. Finite element analysis is carried out for the same roller-flat contact and results are compared with analytical solution given by Hertz. This step is required to check the feasibility of FE procedure. In the second part of the work FE analysis has been carried out for the same applied load and material for all five cases, only the change is rollers are taken hollow. Roller hollowness is ranging from 10% to the hollowness for which bending stress at the inner bore should not exceed endurance limit of the material is taken for the consideration. Flexural fatigue failures occurred in hollow roller when the maximum bending stress at the bore cross the limit of endurance limit of the material. The fatigue cracks always began in the bore of the hollow roller. Those that propagated to the roller surface resulted in surface cracks and spallig and finally it fails the bearing. Around seventy FE analysis are done to generate the large data range. Finally graphical solution has been proposed to identify optimum hollowness irrespective of geometry of bearing and material properties.

2. Analytical study of solid cylindrical roller bearings

In the present work five different cylindrical roller bearing of NU 22 series are selected. First of all load distribution (Fig. 1) is calculated by applying load equal to static load carrying capacity of the bearing and the values of contact pressure, deflection, contact width and von Mises stress induced in the roller-race interface are determined (SKF General Catalogue, 1989; Design Data, 1994; Harris, 2001; Shigley, 1983; Nortron, 2010; I. S. 9202, 2001; Harris & Kotzalas, 2007; Horng, Ju & Cha, 2000; Demirhan & Kanber, 2008; Kania, 2006). Taking modulus of elasticity E = 201330 N/mm^2 and Poission ratio v = 0.277 for the bearing material AISI 52100 steel (Guo & Liu, 2002). These five cylindrical roller bearings are selected in such a way that the size of roller should be in step of 5 mm approximately. So we can get the wide data range of load distribution for further analysis. Considering this point in the

present work 2206, 2210, 2215, 2220 and 2224 bearings are selected for analytical analysis. Contact behavior of all these bearing is studied using Hertz theory.

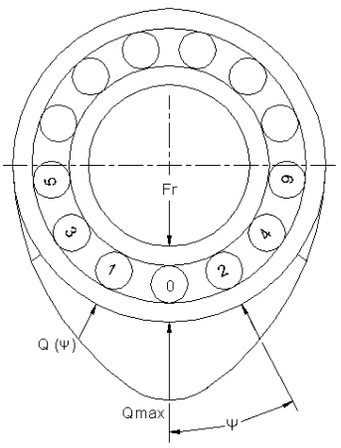

Figure 1. Load distribution in roller bearing

Before executing the FE analysis for cylindrical roller bearing to understand the contact behavior, it is possible to execute the same contact behavior for roller-flat interaction in place of roller-race as shown in Fig. 2. It is very easy to check the contact behavior of roller and flat. To check the contact behavior of roller and flat, if we will take the same diameter of roller which is used in the corresponding roller bearing then contact width will be changed. So comparison of contact behavior of roller and flat with roller-race as in case of bearing is not possible. Using the equation for equivalent diameter in the present work roller diameter is identified in such a way that for the same loading condition contact width of roller and flat interaction will remain same as the interaction of roller with race in bearing. These equivalent diameter of roller is designated by 'Roller 1' for NU 2206 bearing, 'Roller 2' for NU 2210 bearing, 'Roller 3' for NU 2215 bearing, 'Roller 4' for NU 2220 bearing and 'Roller 5' for NU 2224 bearing. Contact interaction between roller and flat plate is shown in Fig. 1, which is a part of the contact between inner-race and roller in the cylindrical roller bearing as described. This contact interaction is studied in detail by analytically using Hertz theory in the present work.

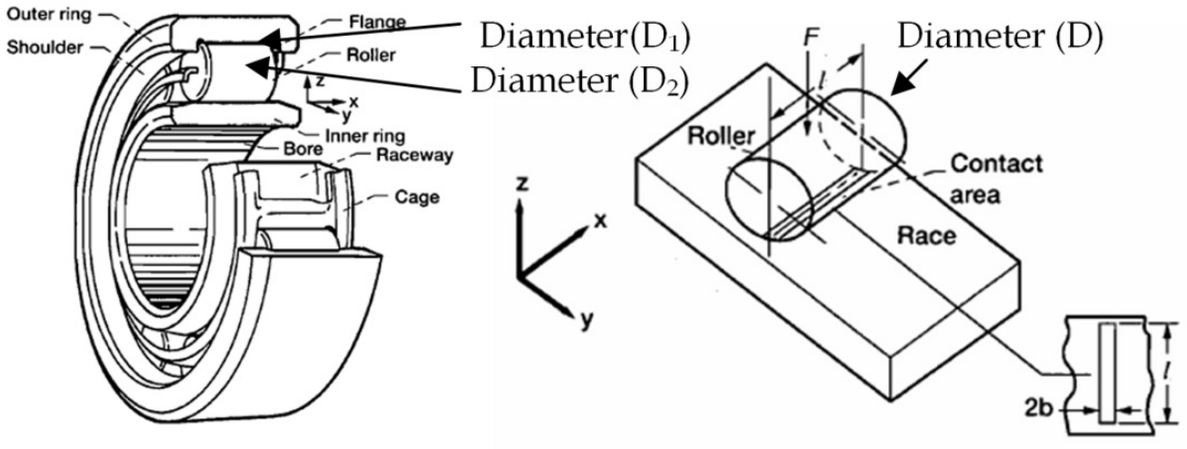

Figure 2. Schematic of contact profile of roller on flat race

Table 1 shows the value of all these analytical results corresponding to roller-flat contact.

Roller position	Load (Q) N	Contact width (b)mm	Contact pressure (p_{max}) N/mm²	von Mises stress (σ_{VM}) N/mm²	Deformation (δ) mm
0	5414.28	0.1321	2175.58	970.31	0.01206
1 & 2	4730.5	0.1235	2033.57	906.97	0.01068
3 & 4	2890.5	0.0965	1589.61	708.97	0.00685
5 & 6	517.68	0.0408	672.72	300.03	0.00146

Table 1. Analytical results for 2206 bearing : Equivalent diameter – 6.62 mm (Roller 1)

Roller Position	Load (Q) N	Contact width (b) mm	Contact pressure (p_{max}) N/mm²	von Mises stress (σ_{VM}) N/mm²	Deformation (δ) mm
0	10397.88	0.1929	2451.83	1093.51	0.01917
1 & 2	9404.92	0.1835	2331.82	1039.99	0.01752
3 & 4	6656.75	0.1544	1961.77	874.95	0.01283
5 & 6	2823.74	0.1005	1277.7	569.86	0.00593

Table 2. Analytical results for 2210 bearing : Equivalent diameter – 8.58 mm (Roller 2)

Roller position	Load (Q) N	Contact width (b) mm	Contact pressure (p_{max}) N/mm²	von Mises stress (σ_{VM}) N/mm²	Deformation (δ) mm
0	21620.59	0.2713	2307.3	1029.05	0.02581
1 & 2	19801.61	0.2596	2208.11	984.81	0.02385
3 & 4	14716.21	0.2238	1903.56	848.99	0.01826
5 & 6	7444.23	0.1592	1353.88	603.83	0.00989

Table 3. Analytical results for 2215 bearing : Equivalent diameter – 12.82 mm (Roller 3)

Roller position	Load (Q) N	Contact width (b) mm	Contact pressure (p_{max}) N/mm²	von Mises stress (σ_{VM}) N/mm²	Deformation (δ) mm
0	50656.34	0.4112	2615.63	1166.57	0.04333
1 & 2	45818.86	0.3911	2487.6	1109.47	0.03959
3 & 4	32430.3	0.329	2092.83	933.4	0.02901
5 & 6	13756.7	0.2143	1363.06	607.93	0.01341

Table 4. Analytical results for 2220 bearing : Equivalent diameter – 17.14 mm (Roller 4)

Roller position	Load (Q) N	Contact width (b) mm	Contact pressure (p_{max}) N/mm²	von Mises stress (σ_{VM}) N/mm²	Deformation (δ) mm
0	73318.39	0.4946	2622.82	1169.78	0.05224
1 & 2	66316.76	0.4704	2494.44	1112.52	0.04773
3 & 4	46938.59	0.3957	2098.59	935.97	0.03497
5 & 6	19911.01	0.2577	1366.81	609.6	0.01616

Table 5. Analytical results for 2224 bearing : Equivalent diameter – 20.56 mm (Roller 5)

The induced von Mises stress in the cylinder/roller is less then the yield strength 1410.17 N/mm² of roller material AISI 52100 steel (Guo and Liu, 2002).

3. FE analysis of solid cylinder and flat contact

3.1. Existing FE models

Since the first mathematical treatment of the contact problem of ideally smooth elastic solids, presented by Hertz in 1882, significant progress has been made in the field of contact mechanics. In particular, the deformation characteristics of semi-infinite elastic media subjected to concentrated and distributed surface traction have been elucidated, and analytical solutions for the contact pressure distributions and subsurface stress fields have been obtained for elastic bodies of different shapes and various interfacial friction conditions (Timoshenko & Godier, 1970). The results of these studies have been invaluable in the design of durable mechanical components, such as rolling element bearings (Komvopoulos & Choi, 1992). Existing FE Models like GW Model (Greenwood & Williamson, 1966), KE Model (Kogut & Etsion, 2002) and JG Model (Jackson & Green, 2005) are studied and finite element analysis for the present case is carried out.

3.2. Finite element analysis details

3.2.1. Model description

In order to validate the relationship of load vs deflection, load vs contact width etc., an FE model of an un-profiled roller contacting a flat plate was set up. A sketch of the problem is presented in Fig. 3.

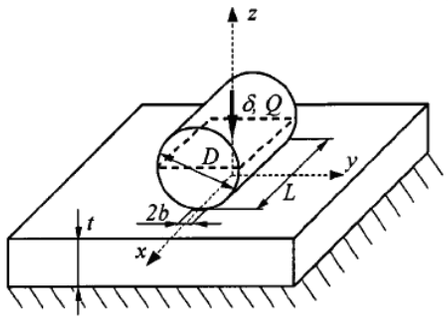

Figure 3. Sketch of roller-plat contact model

A commercial package ANSYS 9.0 was used to solve the non linear contact problem. Initially for Roller 1, first of all three dimensional axis symmetric model was developed to form the single asperity contact between half cylinder and flat plate as shown in Fig. 6. For bearing 2206 taking equivalent diameter of roller as 6.62 mm and length 12mm. Dimensions of flat plat are taken as 12 x 8 x 2 mm^3. The circular surface of cylinder and contact flat surface of plate was discretized by SOLID 185 elements. SOLID185 is used for the 3-D modeling of solid structures. It is defined by eight nodes having three degrees of freedom at each node: translations in the nodal x, y, and z directions see Fig. 4. The element has plasticity, hyperelasticity, stress stiffening, creep, large deflection, and large strain capabilities. It also has mixed formulation capability for simulating deformations of nearly incompressible elastoplastic materials, and fully incompressible hyperelastic materials.

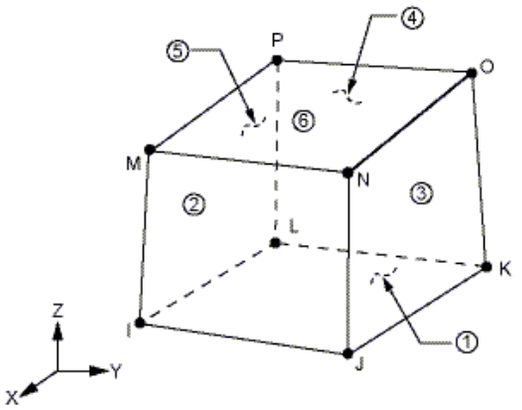

Figure 4. SOLID 185 geometry

3.2.2. Mesh convergence

A converged solution is one that is nearly independent of meshing errors. An extremely coarse mesh would give a very approximate solution, which is far from reality. As the mesh is refined by reducing the size of the elements, the solution slowly approaches an exact solution. It should be noted that, in theory, the solution will not be exact until the mesh size is zero, which is obviously impossible. However, it is possible to fix a tolerance to the solution error and this can be achieved by solving the problem on several meshes. In order to ensure that the solution obtained is as close as possible to reality, solutions should be obtained from several meshes starting with a very coarse mesh and finishing with a very fine mesh. Once these solutions are available, many key quantities can be compared and plotted against mesh densities (or number of points) as shown in Fig. 5.

In order to investigate the convergence of the solutions, all models have been solved with increasing numbers of elements. The elements around the roller contact region are subdivided into number of elements as shown in Fig. 7. Although the stresses and displacements at different regions are investigated in this work the convergence check has been made for only point A as shown in Fig. 7 It is a common point of contact of roller and flat plate where induced von Mises stress should be investigated. The von Mises stress (σ_{VM})

converged with coarse to fine meshes as shown in Fig. 5. The number of elements and nodes of models will increase as size of model will increase.

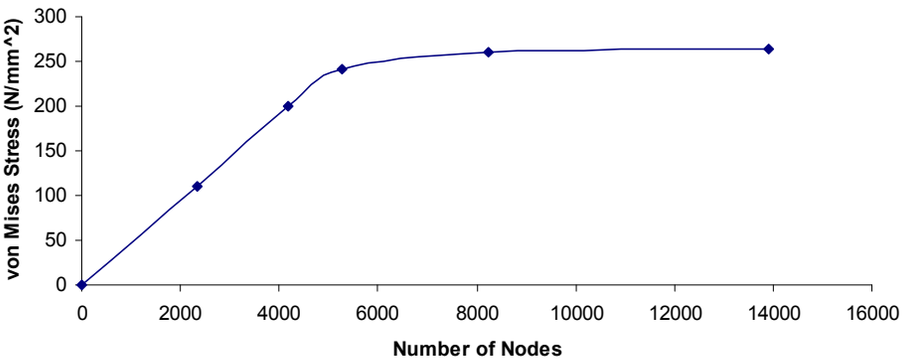

Figure 5. Von Mises stress vs number of nodes

It is very clear from the Fig. 5 that for the last three points value of von Mises stress is approximately same and its value are 242.09 N/mm², 259.94 N/mm² and 263.52 N/mm² for the corresponding values of 0.08, 0.05 and 0.03 element edge length.

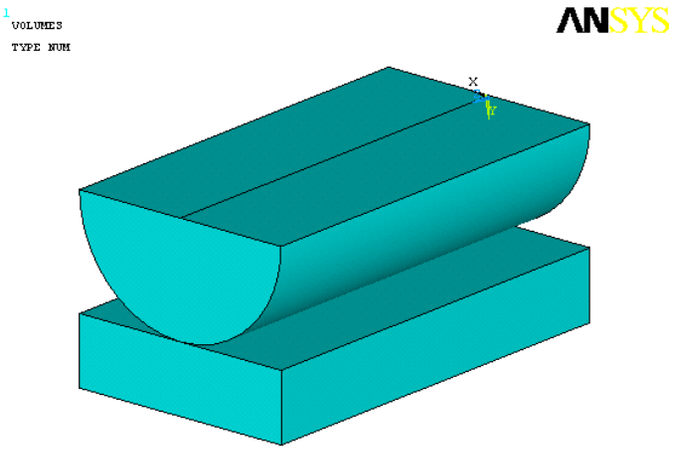

Figure 6. Finite Element Model

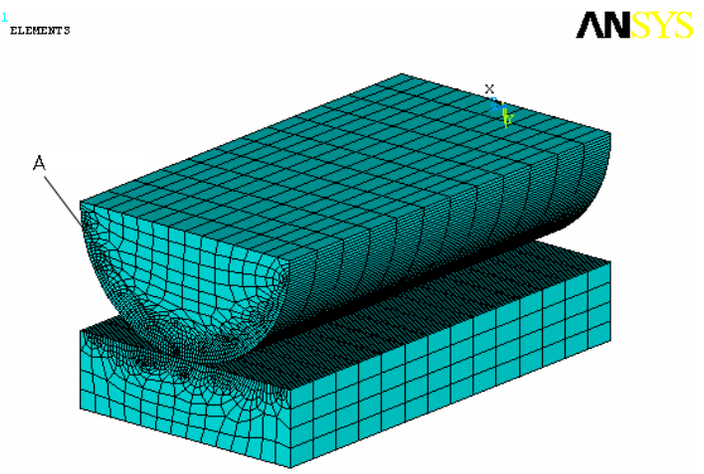

Figure 7. Densely meshed regions of the contact model

The region of most interest is adjacent to the contact interface and has the greatest concentration of elements for lower interferences. Away from the contact region, the mesh becomes coarser to minimize the computational efforts. In the present all FE models in contact region element edge length is taken as 0.08 and in other area it is taken as 0.5, the details of which is shown in Fig 8. The total numbers of elements generated are 14120 and nodes generated are 16977 for this model.

3.2.3. Contact model

In order to create contact models in ANSYS, a contact pair of elements must be created a contact element and a target element. ANSYS has general guidelines as to what line, surface, or volume these elements should be applied. Perhaps the most critical feature is the mesh size. For example, a large target element size and very fine contact element will not work. The sizes of the contact and target elements should be fairly close to one another. It is possible to get a solution to converge, but the results will most likely be incorrect. That is why there is a densely meshed region in both the bottom part of the half-cylinder and on the surface of the block shown in Fig. 8.

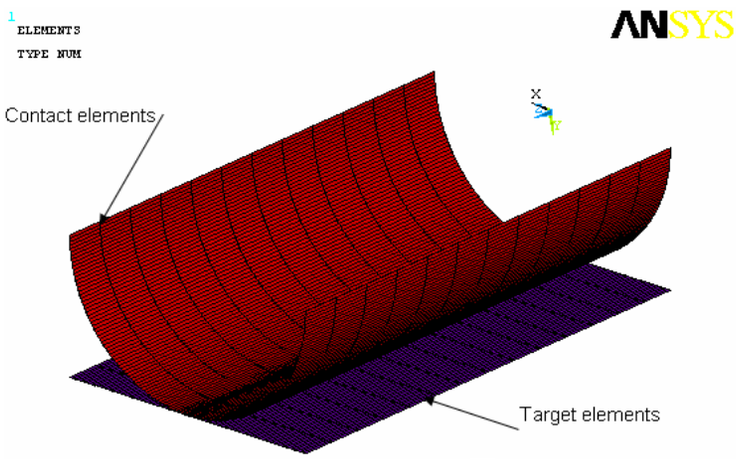

Figure 8. Contact and target elements

3.2.4. Boundary condition and application of pressure

The boundary conditions are presented in Fig. 9. The nodes on the bottom surface of the flat plat all degree of freedoms are restricted and rigidly constrained from translating in the x, y and z direction. Where as on top surface of half cylinder uniform pressure of 68.16 N/mm² is applied which is related with Qmax (5414.28 N) for bearing no. 2206

3.2.5. Solutions

The solutions have been carried out by means of a PC. The hardware configuration consists or an Intel Pentium IV 2.53 GHz CPU with 1 GB of RAM. The models were solved in round 25 minutes to 7 hours. All models have been solved as 3D static with Newton Raphson option.

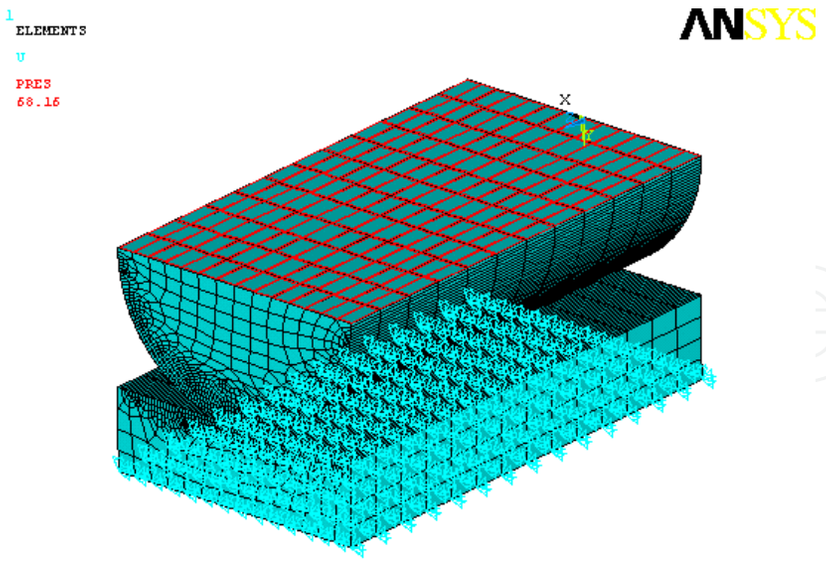

Figure 9. Applied pressure and boundary condition

3.2.6. Evaluation of the finite element model

To examine the appropriateness of the finite element mesh and modeling assumptions, such as the dimensions and fineness of the mesh and the imposed boundary conditions, finite element results for an elastic half-space indented by a rigid cylindrical asperity were compared with analytical results for line contacts. The FE model was first verified by comparing its output with the analytical results of the Hertz solution in the elastic regime. The verification included the contact pressure, contact stresses, deformation and contact width. For the evaluation of Finite Element Model initially von Mises stress criteria is taken for the consideration because it is the final output of analytical study as discussed in section 2. Also it is an important stress which should remain within limit with respect to yield stress of the material. Figure 10 shows the contour plot of von Mises stress for the applied load of 5414.28 N. As it is clear from the figure that at contact zone induced stress is higher which is marked by red colour. Figure 11 shows the detail view of contact zone with node numbers. Value of von Mises stress is to be identifying for the node no 5258 which is on contact surfaces and it is 1031.1 N/mm^2. Whereas analytical result gives 970.31 N/mm^2 (Table 1). Thus the von Mises stress of FE model differs from the Hertz solution by 5.8% which is acceptable for the present analysis. The small differences between analytical and FEA solutions near the contact edge may be attributed to the fineness of the mesh. The favorable comparison of the results illustrates the suitability of the finite element model for the present analysis involving only global variables, such as von Mises stress, contact pressure, contact width and deformation.

Figure 12 shows the contour plot for shear stress distribution. It is clear from the FE analysis that value of induced shear stress is 457.88 N/mm^2 and analytical result gives 485.16 N/mm^2 with the percentage error of 5.6 % only.

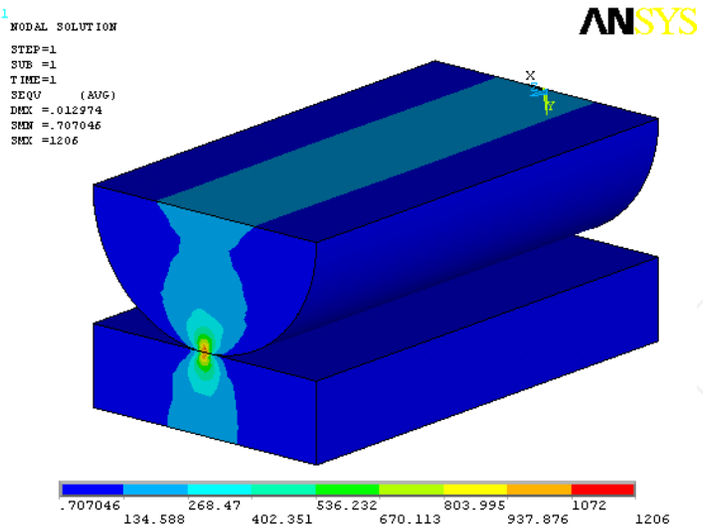

Figure 10. von Mises stress distribution over solid cylinder-flat

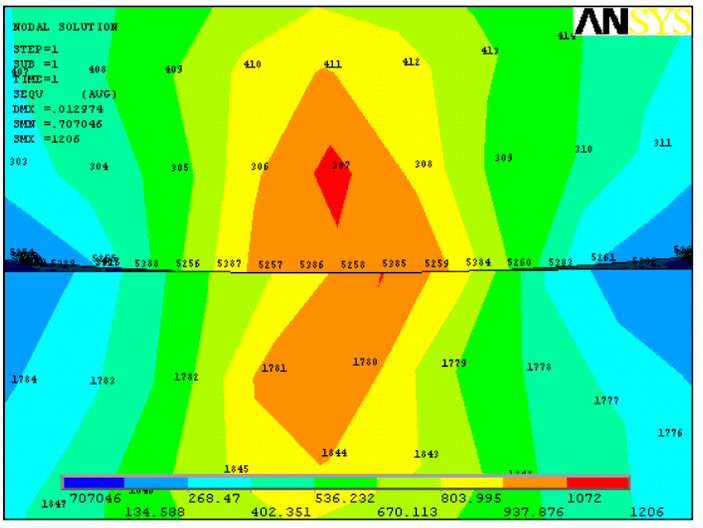

Figure 11. Detail of contact zone for von Mises stress distribution

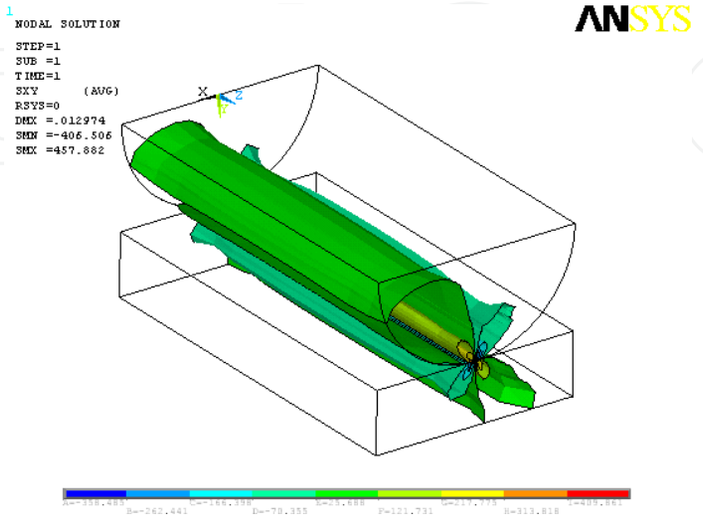

Figure 12. Contour plots for shear stress

Now using similar contact model and boundary conditions FE analysis has been carried out for all five rollers. Applied loads are taken as per the calculated load distribution among the rollers. Table 6 shows the validation of meshing scheme employed by comparing the analytical results with FEA.

Figure 13 to 16 shows the graphical comparison of Table 6. Four important parameters von Mises stress, Contact Pressure, Deformation and Contact Width are plotted for different applied load.

Load (N)	Von Mises stress, σ_{VM} (N/mm^2)		Contact width, b (mm)		Contact pressure, p (N/mm^2)		Deformation, δ (mm)	
	Analytical	FEA	Analytical	FEA	Analytical	FEA	Analytical	FEA
Roller 1								
5414.28	970.31	1031.1	0.1321	0.1412	2175.58	2034.5	0.01206	0.01288
4730.5	906.97	958.92	0.1235	0.1322	2033.57	1898.2	0.01068	0.01148
2890.5	708.97	719.39	0.0965	0.1066	1589.61	1437.9	0.00685	0.00742
517.68	300.03	242.09	0.0408	0.0467	672.72	587.2	0.00146	0.00184
Roller 2								
10397.88	1093.51	1083.7	0.1929	0.2097	2451.83	2255.4	0.01917	0.02028
9404.92	1039.99	1018.9	0.1835	0.2003	2331.82	2136	0.01752	0.0186
6656.75	874.95	840.21	0.1544	0.1726	1961.77	1754.5	0.01283	0.01376
2823.74	569.86	519.65	0.1005	0.1218	1277.7	1053.9	0.00593	0.006469
Roller 3								
21620.59	1029.05	1110	0.2713	0.2991	2307.3	2092.5	0.02581	0.02643
19801.61	984.81	1050.2	0.2596	0.2877	2208.11	1992.4	0.02385	0.02451
14716.21	848.99	914.4	0.2238	0.2529	1903.56	1684.6	0.01826	0.01899
7444.23	603.83	616.54	0.1592	0.1879	1353.88	1146.5	0.00989	0.01057
Roller 4								
50656.34	1166.57	1245.6	0.4112	0.4659	2615.63	2308.2	0.04333	0.04357
45818.86	1109.47	1176.8	0.3911	0.4466	2487.6	2177.8	0.03959	0.04
32430.3	933.4	957.3	0.329	0.3860	2092.83	1783.4	0.02901	0.02989
13756.7	607.93	592.31	0.2143	0.2723	1363.06	1072.4	0.01341	0.01442
Roller 5								
73318.39	1169.78	1237.3	0.4946	0.5677	2622.82	2285	0.05224	0.05235
66316.76	1112.52	1174.7	0.4704	0.5442	2494.44	2155.9	0.04773	0.04811
46938.59	935.97	963.4	0.3957	0.4706	2098.59	1764.6	0.03497	0.03604
19911.01	609.6	582.93	0.2577	0.3306	1366.81	1065.4	0.01616	0.01758

Table 6. Validation of meshing scheme employed

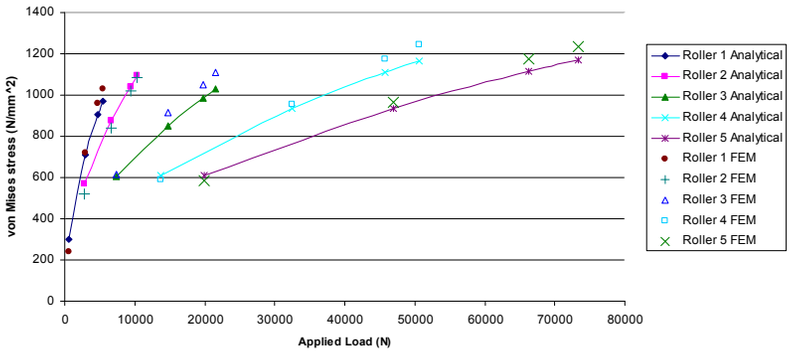

Figure 13. von Mises stress vs Applied load

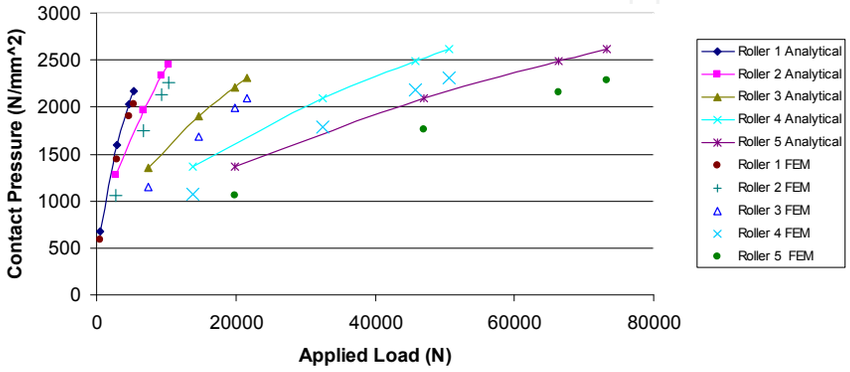

Figure 14. Contact Pressure vs Applied load

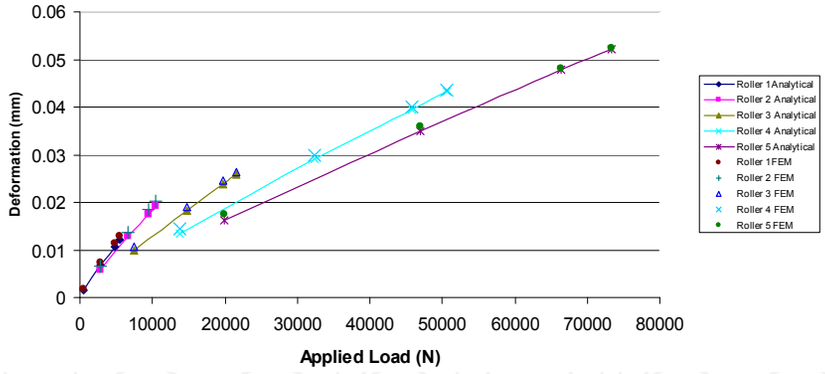

Figure 15. Deformation vs Applied load

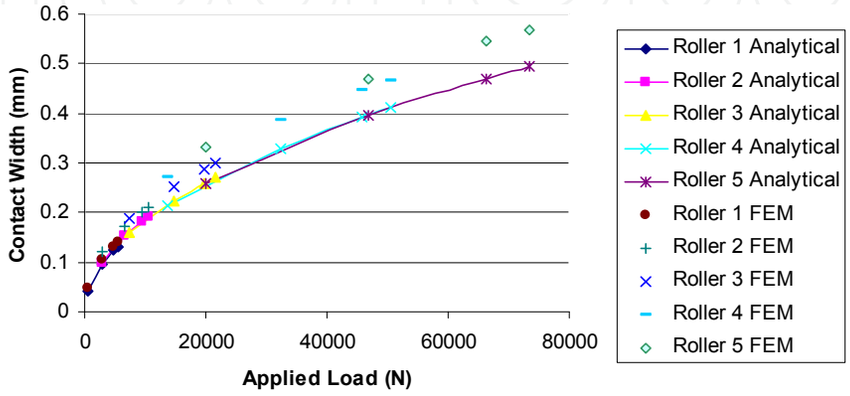

Figure 16. Contact Width vs Applied load

3.2.7. Summary of FE analysis

The finite element method was used to analyze the contact mechanics aspects of nominally flat single-asperity surfaces and to identify the effect of important parameters like von Mises stress, contact pressure, contact width and deformation for the given load. On the basis of the presented results, the following major conclusions can be drawn.

The smaller error in the FE model is attributed to overall balance (static equilibrium) enforced by the FEM package. The smaller differences between analytical and FEA solutions near the contact edge may be attributed to the fineness of the mesh.

On the basis of the results discussed, it may be concluded that the finite element configuration shown in Fig. 10 and the invoked modeling approximations are acceptable for the purpose of the present analysis.

Figure 14 to 17 shows that the agreement between analytical and finite element results from different rollers and various load is appreciably good. The maximum disagreement between the FEA value and analytical values occurs at the lowest applied load. The accord between the FEA and analytical results gets progressively better as higher applied load. Thus smaller the interference the smaller number of contact elements are in effect, leading to a large error and visa versa.

4. Finite element analysis for hollow roller and flat contact

4.1. Finite element model

Different hollowness percentage ranging from 10% to 80% (in step of 10%) has been investigated for Roller 1 of diameter 6.62 mm which is equivalent of 8 mm diameter roller co-relate with bearing 2206. Figure 17 shows the finite element model for 40 % hollowness. Same surfaces as taken in the contact model of solid roller and flat i.e. outer surface of roller and top surface of flat plate are selected for contact element and target element respectively.

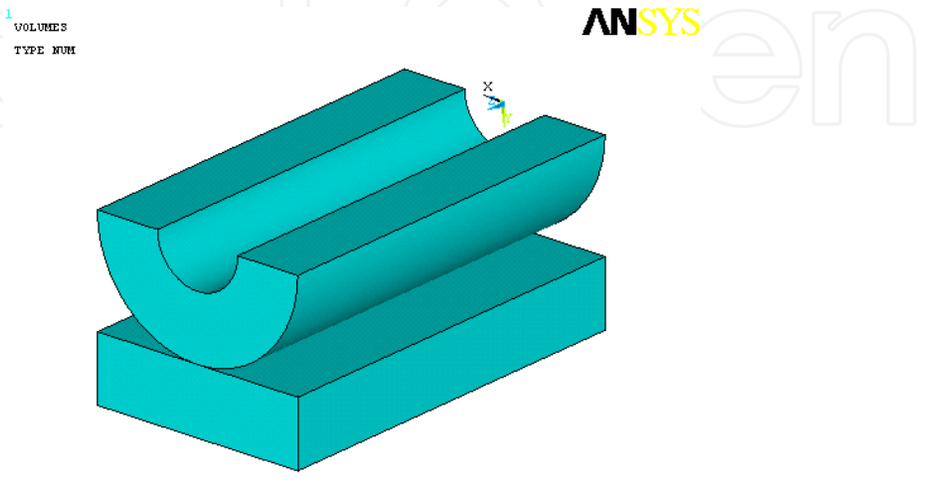

Figure 17. Finite element model for 40% Hollowness

4.2. Meshing

Now in this case also for the contact surface element edge length is taken as 0.08. Also as discussed by Murthy & Rao (1983) that, in addition to the contact stresses at the outer contact zone, the hollow specimens are subjected to tangential stresses (bending stress) at inner surface. Thus for the inner surface element edge length should be high and is taken as 0.08 as shown in Fig. 18. For other remaining area it is taken as 0.5.

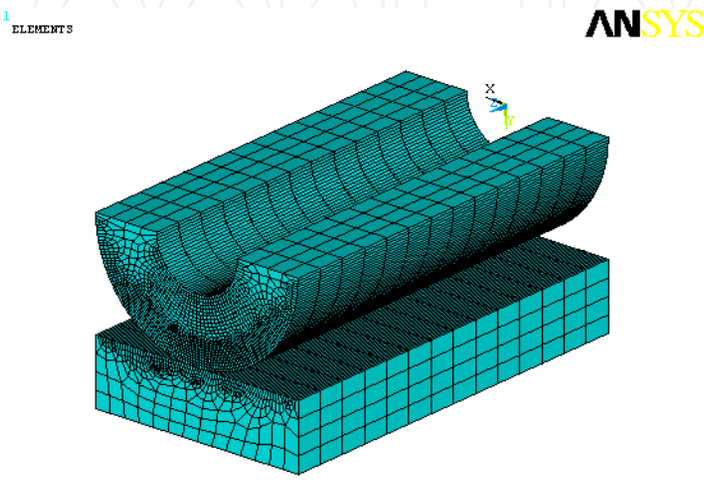

Figure 18. Densely meshed regions of the contact model of hollow roller and flat

Same boundary condition and pressure is applied as discussed in section 3.2.4. For each hollowness 10% to 80%, FE model is developed as shown in Fig. 19, maximum applied load 5414.28 N is taken and results are observed.

5. Results and discussion

Due to thin section very less material is available to resist the force so von Mises stress is increase after 60% hollowness. Also at this stage plastic deformation will take place and failure will occur due to permanent deformation, which is not desirable and should be avoided.

An added criterion for evaluation in a bearing with hollow rollers is the roller bending stress. To evaluate the life integrals, the value of the fatigue limit stress must be known for the bearing component material. This can be determined by endurance testing of bearings or selected components. Performance analyses were conducted, using the von Mises stress as the fatigue failure-initiating criterion. Based on this subsequent study fatigue limit stress for bearing material AISI 52100 is 684 N/mm^2 (Harris and Kotzalas, 2007). From Table 7 it is very clear that bending stress is continuously increase from 377.07 N/mm^2 to 1721.4 N/mm^2 as hollowness increase from 10% to 80% respectively. But the practical limit of this stress is 684 N/mm^2. So the hollowness should be restricted upto 52% which is clear from Fig. 20.

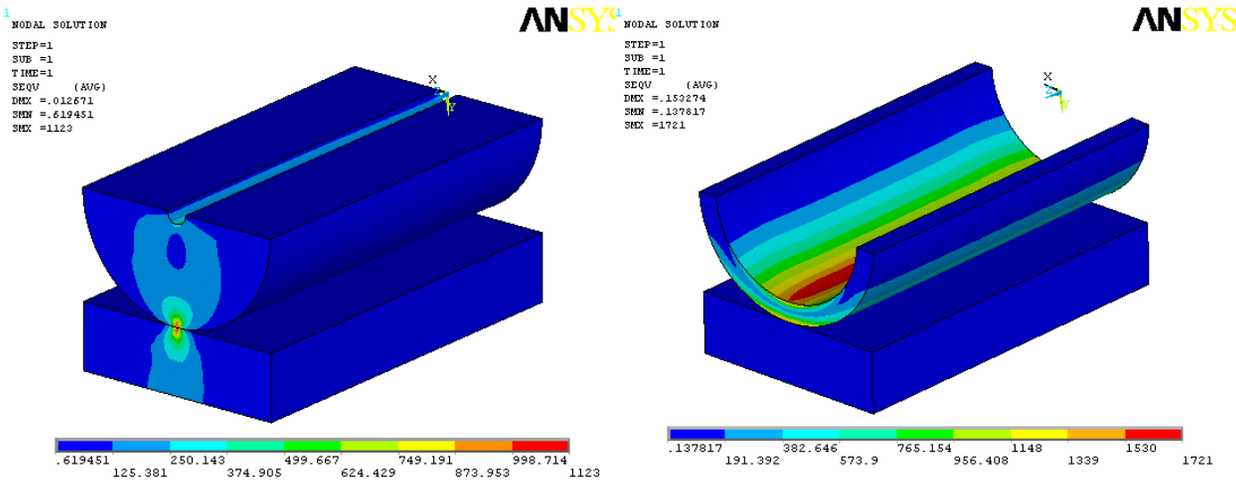

(a) 10% hollowness (b) 80% hollowness

Figure 19. von Mises stress plots for hollow roller

Hollowness %	Contact pressure (N/mm^2)	von Mises stress (N/mm^2)	Bending stress (N/mm^2)	Deformation (mm)
10	1901	952.92	377.07	0.01253
20	1812.3	895.99	422.55	0.01264
30	1679.6	843.84	463.1	0.01345
40	1536.3	785.46	539.91	0.01517
50	1391.9	741.49	650.03	0.01885
60	1247.1	704.71	822.71	0.02663
70	1093.3	832.79	1123.8	0.04516
80	897.31	1379.1	1721.4	0.10102

Table 7. Values of parameters for different hollowness for Roller 1

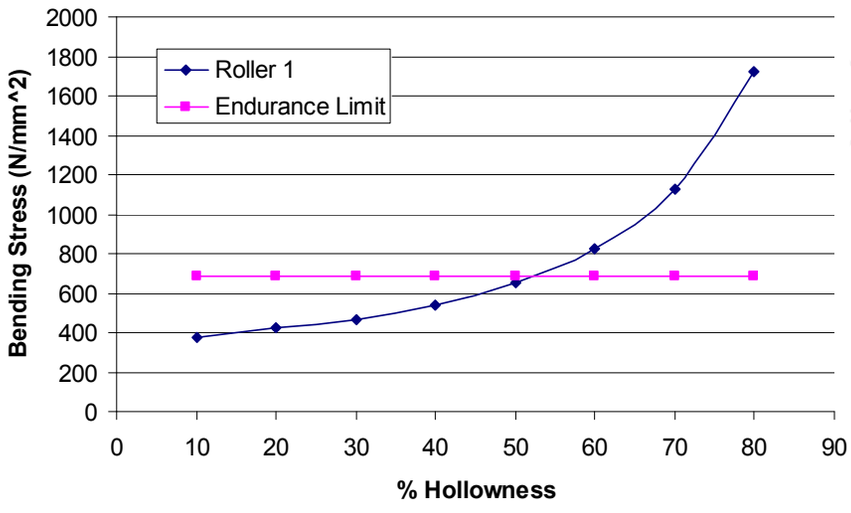

Figure 20. Bending stress vs Hollowness for Roller 1

Thus for the present case of Roller 1, for the applied load of 5414.28 N the % hollowness of the hollow roller should not exceed 52%, otherwise induced stress at the bore of the roller will increase beyond the endurance limit and cause fatigue failure of roller.

Great care must be given to the smooth finishing of the inside surface of a hollow roller during manufacturing as the stress raisers that offer due to poorly finished inside surface will reduce the allowable roller hollowness ratios still further than indicated by Fig. 20.

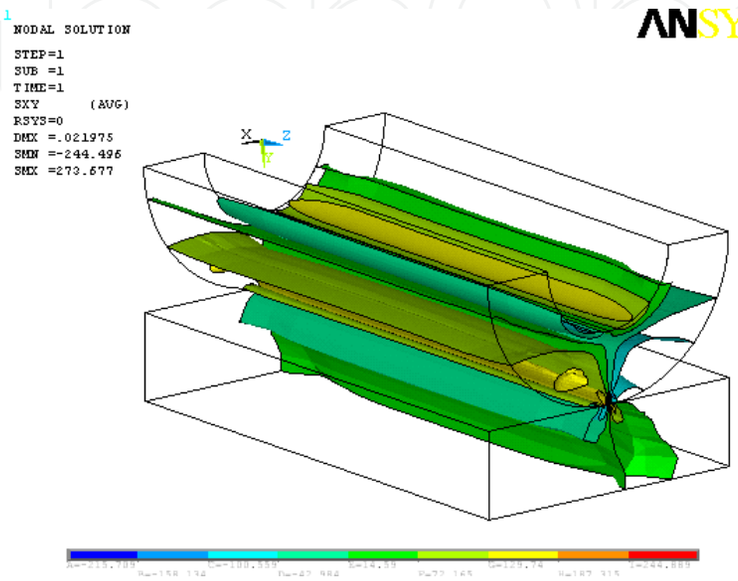

Figure 21. Contour plot for maximum shear stress for hollow roller

Figure 21 shows the contour plot of maximum shear stress for 52% hollowness. The induced shear stress is 273.68 N/mm^2 which is approximately half than the shear stress induced in solid roller for the same load of 5414.28 N. Thus reduction in shear stress gives improvement in fatigue life of bearing.

Figure 22 to 25 shows the effect of hollowness on different parameters.

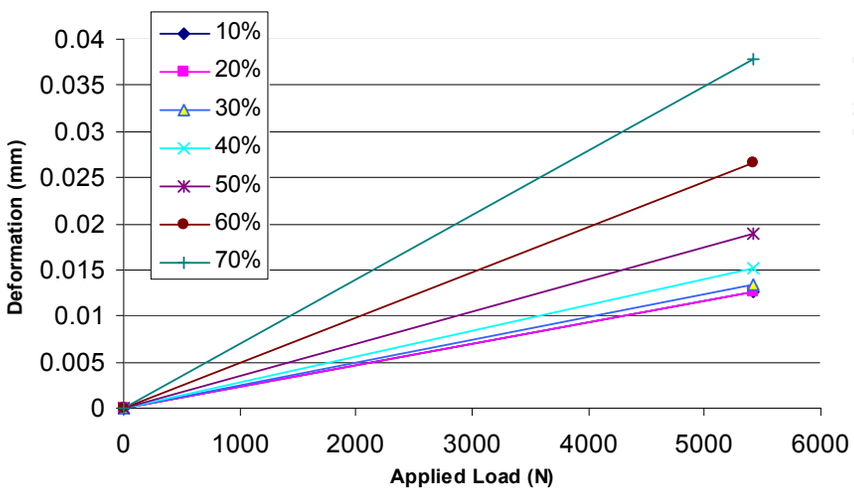

Figure 22. Effect of hollowness on the deformation for same applied load

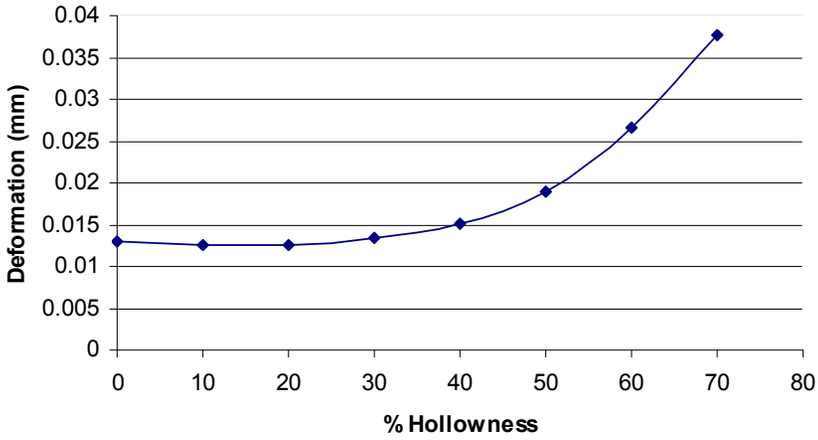

Figure 23. Deformation vs Hollowness

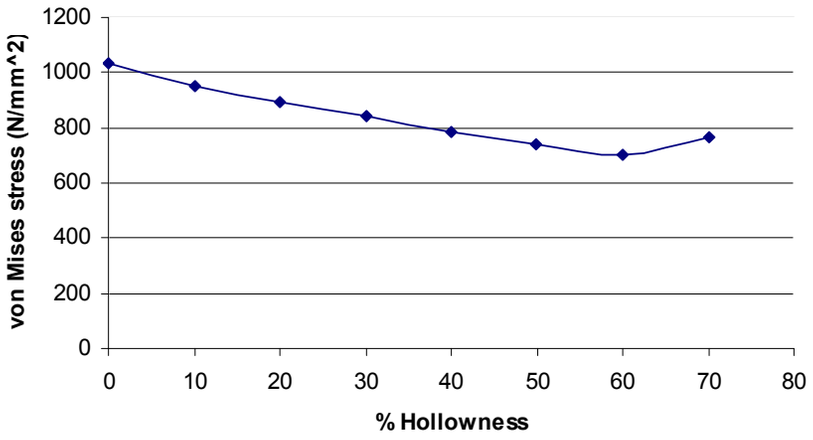

Figure 24. Mises stress vs Hollowness

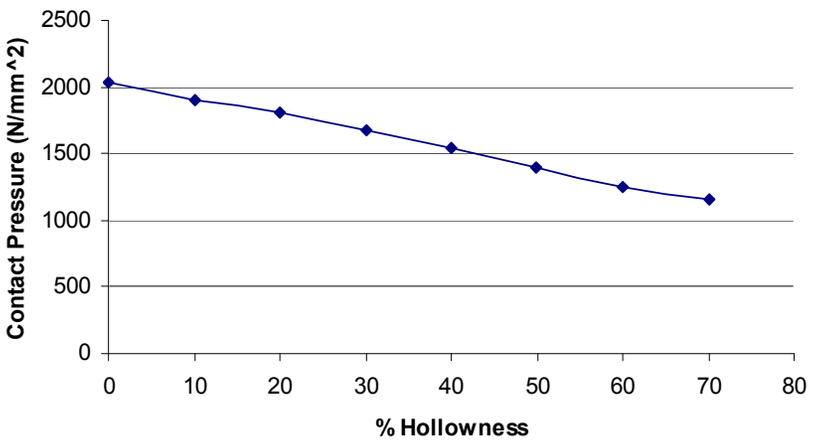

Figure 25. Contact pressure vs Hollowness

The term "hollowness" as referred to here for the rollers in the ratio of the inner diameter to the outer diameter expressed as a percentage and is an important parameter in the design of the hollow roller bearing. It determines not only the overall bearing stiffness but also the amount of preload most desirable, the bearing's load capacity and its life. In fact, hollowness

is a control parameter used to optimize the bearing design. In the present case of Roller 1, load is applied in such a way that induced bending stress at inner bore should cross endurance limit of the material i.e. 684 N/mm^2 for each hollowness. Result of FE analysis is shown in Fig. 26. The roller hollowness values from 10% to 80% have been analyze by Finite Element as discuss above for Roller 1 and the roller load, deflection and stress curves of Fig. 27 have been developed. The dotted line across these curves show the points of constant maximum roller bore stress for values of 684 N/mm^2.

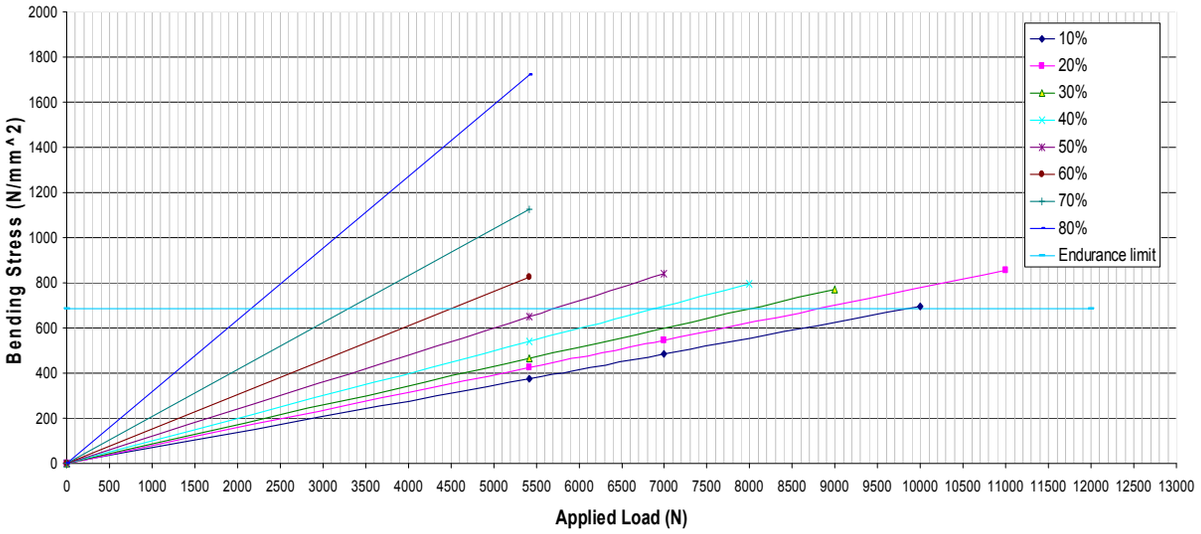

Figure 26. Bending stress crosses the endurance limit for different hollowness

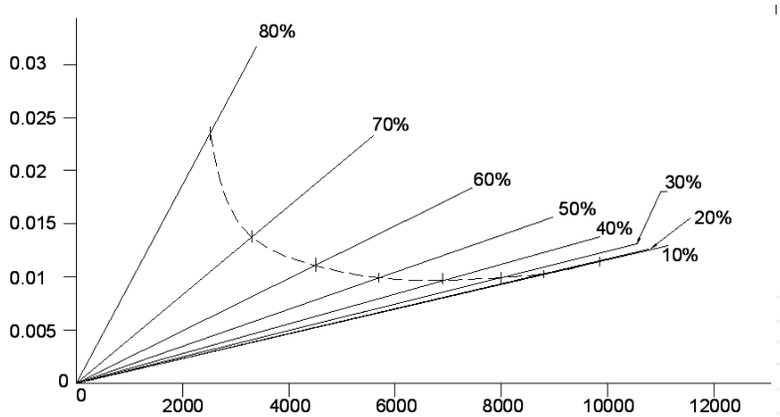

Figure 27. Relationship between the roller hollowness, Deflection and bore stress for 6.62 mm diameter roller

Corresponding to each roller hollowness value, there is a specific optimum load for each bearing design, which is indicated in Table 8.

Figure 27 gives the best solution to find the optimum hollowness for verities of load. But this is not the final solution, because solution given in Fig. 27 is only applicable for Roller 1 i.e. equivalent roller of bearing 2206. As bearing/roller geometry will change again same procedure of FE analysis should be carried out and again optimum hollowness is to be

identified. Thus similar analysis can also be carried out for remaining four rollers to find the optimum hollowness and results are given in Table 9. For each roller these analyses have been carried out upto the hollowness where induced bending stress should just cross the endurance limit.

% Hollowness	Max. Applied Load (N)
10	9850
20	8800
30	8000
40	6900
50	5700
60	4500
70	3300
80	2520

Table 8. Maximum applied load for different hollowness for Roller 1

Roller no	Maximum Load (Q_{max}) N	% Hollow-ness	Contact pressure (N/mm^2)	von Mises stress (N/mm^2)	Bending stress (N/mm^2)	Deformation (mm)
Roller 2	10397.88	10	2153.5	1067.8	500.59	0.0195
		20	1984.2	1045.7	548.37	0.02
		30	1812.5	969.11	599.86	0.02149
		40	1652.5	900.87	693.55	0.02461
Roller 3	21620.59	10	1917.9	975.09	468.32	0.026
		20	1769.9	909.63	491.53	0.02671
		30	1629.6	855.49	538.21	0.02871
		40	1484	818.1	619.64	0.03284
		50	1324.6	804.27	746.49	0.04103
Roller 4	50656.34	10	2126.9	1094.9	620.35	0.0428
		20	1951.7	1021.8	634.68	0.04448
		30	1802.2	984.04	689.2	0.04793
Roller 5	73318.39	10	2105.2	1084.6	633.57	0.05157
		20	1922	1009.9	640.66	0.05374
		30	1820.2	993.23	692.28	0.05704

Table 9. Values of parameters for different hollowness for Roller 2, 3, 4 & 5

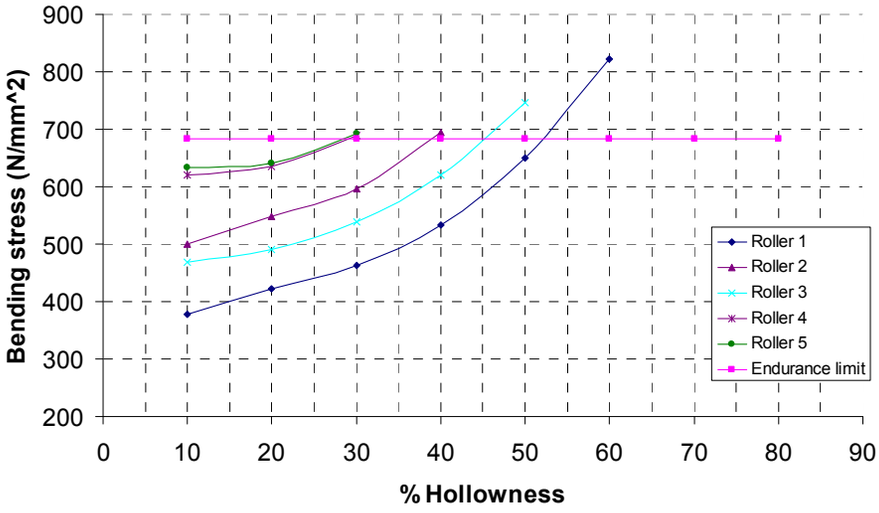

Figure 28. Comparison of hollowness for different rollers

From Fig. 28 it is clear that for

Roller 1 optimum hollowness should be 52% for the applied load of 5414.28 N,
Roller 2 optimum hollowness should be 39% for the applied load of 10397.88 N,
Roller 3 optimum hollowness should be 45% for the applied load of 21620.59 N,
Roller 4 optimum hollowness should be 29% for the applied load of 50656.34 N,
Roller 5 optimum hollowness should be 28% for the applied load of 73318.39 N.

It is very clear from the results and discussion of all five rollers that optimum value of hollowness is dependent on magnitude of applied load, bearing geometry i.e. diameter and length of roller and mechanical properties of material used. If the value of applied load will increase than hollowness should be reduced to maintain the bending stress within endurance limit of the material. Change in bearing geometry will change the applied pressure and resulted into change in hollowness. Thus the solution given in Fig. 26 and 27 is not a generalized solution and it can not be applicable to any bearing geometry for any load. It is applicable to specific type of bearing and for specific load only respectively. If applied load will change one can't use the results shown in Fig. 28 and lengthy FE procedure should be again carried out to get the result in the form of hollowness.

5.1. Generalized graphical solution

To find the optimum hollowness for any material and for any applied load irrespective of bearing geometry, in the present work large data are generated by FE analysis. To get the generalized solution FE analysis for the hollowness percentage ranging from 1% to 95% (after 95% ANSYS solution was not supported) is carried out and following Table 10 has been developed. This table shows the values of bending stress corresponding to the applied pressure.

Table 10 is presented in graphical form in Fig. 29. This diagram shows the value of bending stress for different applied pressure with respect to hollowness ranging from 1% to 95%.

Applied pressure (N/mm²)	Bending Stress (N/mm²)											
	1%	5%	10%	20%	30%	40%	50%	60%	70%	80%	90%	95%
99.06	515.11	526	633.57	640.66	692.28							
98.52	497.6	512.3	620.35	634.68	689.2							
86.56	441.46	450.112	500.59	548.37	599.86	693.55						
78.3	419.68	418.9	452.84	496.14	542.76	627.65						
76.66	371.8	401.3	468.32	491.53	538.21	619.64	746.49					
70.21	344.029	359.13	429	450.31	493.08	567.54	683.78					
68.16	330.68	347.21	377.07	422.55	463.1	539.91	650.03	822.71	1123.8	1721.4	3365	4653.6
59.55	303.71	309.66	329.92	369.25	404.64	471.74	567.96	718.81				
55.42	277.1	282.64	321.12	351.66	384.46	444.33						
52.18	263.5	273.95	319.16	334.9	366.59	422.04	508.42					
36.39	189.23	192.867	201.72	225.7	247.51	288.52	347.05	439.33				
26.39	129.311	138.475	161.84	169.76	185.62	213.61	257.35					
23.51	112.848	124.6	136.5	149.44	163.28	188.71						
6.52	33.9	34.88	36.36	40.636	44.509	51.777	62.158	78.697				

Table 10. Value of bending stress corresponding to the applied pressure

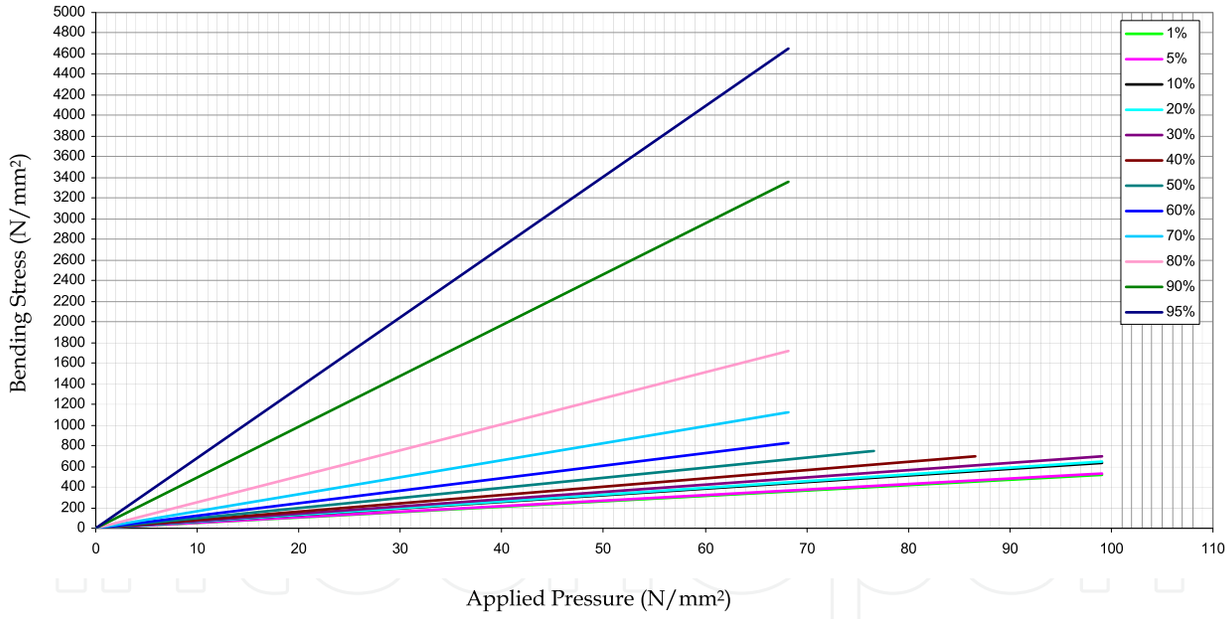

Figure 29. Bending stress vs applied pressure for different hollowness

6. Conclusion

In case of solid roller bearing induced sub-surface stresses are the limiting criteria for the fatigue life of bearing whereas for hollow roller bearing bending stress is the limiting criteria. The bending stresses on the internal diameter of the roller in the plane of the loading forces are the most critical for destructions. In the present work graphical solution was developed to determine optimum hollowness of cylindrical roller bearing for which

induced bending stress should be within the endurance limit of the material. Figure 29 shows the generalized diagram for bending stress vs applied pressure. Following are the major outcomes from this diagram.

For the same value of applied pressure, Fig 29 shows that there is very small variation in the value of bending stress by increase the hollowness from 10% to 30%.

If the hollowness increases from 1% to 95% the slop of line will also increase accordingly.

The durability of the bearings with hollow rollers operating on cycles not exceeding the maximum permitted level of bending stresses can be substantially greater than the durability of similar bearings with solid rollers.

For the applied load on equivalent size of roller initially applied pressure is to be calculated. As per the endurance limit of the material used and calculated applied pressure optimum hollowness can be identified from the diagram.

For the particular hollowness diagram gives the maximum limit of applied pressure and hence applied load. The developed graphical solution can be applicable for any material of bearing.

Author details

P.H. Darji
Department of Mechanical Engineering, C. U. Shah College of Engineering & Technology, Surendranagar, India

D.P. Vakharia
Department of Mechanical Engineering, S.V. National Institute of Technology, Surat, India

7. References

Bamberger, E. N., Parker, R. J. and Dietrich, M. W., 1976, "Flexural Fatigue of Hollow Rolling Elements," NASA TN D – 8313, Washington.

Bhateja, C. P. and Hahn, R. S., 1980, "A Hollow Roller Bearing for Use in Precision Machine Tools," Annals of the CIRP, 29, 1, pp. 303 – 307.

Darji, P. H. and Vakharia, D. P., (2008), "Determination of Optimum hollowness for hollow cylindrical rolling element bearing", Proceedings of ASME 2008 International Mechanical Engineering congress and exposition, Boston, Massachusetts, USA, Oct 31-Nov 6, Paper No. IMECE2008-67294. ISBN: 978-0-7918-4873-9

Demirhan, N. and Kanber, B. (2008) Stress and Displacement Distributions of Cylindrical Roller Bearing Rings Using FEM. Taylor & Francis, Mechanics Based Design of Structures and Machines, 36, 86 – 102. ISSN : 1539 – 7734.

Design Data (1994). PSG College of Technology, Coimbatore.

Greenwood, J. A. and Williamson, J. B. P. (1966) Contact of Nominally Flat Surfaces. Proc. R. Soc. London, Ser A. 295, 300 – 319. ISSN 1471-2946.

Guo, Y. B. and Liu, C. R. (2002) Mechanical Properties of Hardened AISI 52100 Steel in Hard Machining Processes. Tran. ASME, J. Manf. Sci. & Engg., 124, 1 – 9. ISSN 1087-1357.

Harris, T. A. (2001) Rolling Bearing Analysis. , 4th ed, John Wiley & Sons, New York. ISBN 0-471-35457-0

Harris, T. A. and Aaronson, S. F., 1967, "An analytical investigation of cylindrical roller bearings having annular rollers," Tribology Transactions, 10, pp. 235 – 242. ISSN 1040-2004.

Harris, T. A. and Kotzalas, M. N. (2007) Rolling Bearing Analysis - Advanced Concepts of Bearing Technology. 5th ed., Taylor & Francis, Boca Raton. ISBN 10: 0-8493-7182-1.

Hong, L. and Jianjun L., 1998, "Analysis of Contact Problems on Hollow Cylindrical Rollers", Tribology, 120, pp. 134 – 139. ISSN 1004-0595.

Horng, T. L, Ju, S. H. and Cha, K. C. (2000) A Deformation Formula for Circular Crowned Roller Compressed Between Two Flat Plates. Tran. ASME, J. Tribol, 122, 405 – 411. ISSN 0742-4787.

I. S. 9202 (2001) Specification for Cylindrical Rollers. Edition 1.1.

Jackson, R. L. and Green, I. (2005) A Finite Element Study of Elasto-Plastic Hemispherical Contact Against a Rigid Flat. Tran. ASME, J. Tribol, 127, 343 – 354. ISSN 0742-4787.

Kania, L. (2006) Modeling of Rollers in Calculation of Slewing Bearing with the use of Finite Elements. Int. J. Mechanism and Machine Theory, 41, 1359 – 1376. ISSN 0094-114X.

Kogut, L. and Etsion, I. (2002) Elastic-Plastic Contact Analysis of a Sphere and a Rigid Flat. Tran. ASME, J. Tribol, 69, 657 – 662. ISSN 0742-4787.

Komvopoulos, K. and Choi, D. –H. (1992) Elastic Finite Element Analysis of Multi-Asperity Contacts. Tran. ASME, J. Tribol, 114, 823 – 831. ISSN 0742-4787.

Murthy, C.S.C. and Rao, A. R. (1983) Mechanics and Behaviour of Hollow Cylindrical Members in Rolling Contact. Wear, 87, pp. 287 – 296. ISSN 0043-1648.

Nortron, R. L. (2010) Machine Design An Integrated Approach. 2nd ed., Pearson Education, Singapore. ISBN 978-81-317-0533-9.

SKF General Catalogue 4000/ IIE (1989) W. Germany. Reg : 47.23000.

Shigley, J. E. (1983) Mechanical Engineering Design. 1st ed, McGraw-Hall Singapore. ISBN 0-07-100292-9.

Somasundar, H. V. and Krishnamurthy, R., 1984, "Surface Durability of Tufftrided Rolling Elements," Wear, 97, pp. 117 – 127. ISSN 0043-1648.

Timoshenko S. P. and Godier J. N. (1970) Theory of Elasticity. 3rd ed., McGraw-Hall Singapore. ISBN : 0-07-085805-5.

Yangang, W., Yi, Q., Raj, B. and Qingyu, J., 2004, "FE analysis of a novel roller form : A deep end cavity roller for roller type bearings," Elsevier, Journal of Materials Processing Technology, 145, pp. 233 – 241. ISSN 0924-0136.

Zhao, H., 1998, "Analysis of Load Distributions within Solid and Hollow Roller Bearings", ASME J. Tribol., 120, pp. 134 – 139. ISSN 0742-4787.

IntechOpen